

# The QCD description of diffractive $\rho$ meson electroproduction

A. D. Martin, M. G. Ryskin<sup>1</sup> and T. Teubner

Department of Physics, University of Durham, Durham, DH1 3LE, UK.

## Abstract

We critically review the QCD predictions for the cross sections  $\sigma_L$  and  $\sigma_T$  for diffractive  $\rho$  meson electroproduction in longitudinally and transversely polarised states in the HERA energy region. We show that both perturbative and non-perturbative approaches which involve convolution with the  $\rho$  meson wave function predict values of  $\sigma_T$  which fall-off too quickly with increasing  $Q^2$ , in comparison with the data. We present a perturbative QCD model based on the open production of light  $q\bar{q}$  pairs and parton-hadron duality, which describes all features of the data for  $\rho$  electroproduction at high  $Q^2$  and, in particular, predicts a satisfactory  $Q^2$  behaviour of  $\sigma_L/\sigma_T$ . We find that precise measurements of the latter can give valuable information on the  $Q^2$  behaviour of the gluon distribution at small  $x$ .

---

<sup>1</sup>Permanent address: Laboratory of Theoretical Nuclear Physics, St. Petersburg Nuclear Physics Institute, Gatchina, St. Petersburg 188350, Russia.

# 1. Introduction

The results of the measurements of  $\rho$  meson electroproduction,  $\gamma^*p \rightarrow \rho p$ , are intriguing. These are coming from the H1 [1] and ZEUS [2, 3] experiments at the HERA electron-proton collider, and should be considered in conjunction with the earlier measurements of NMC [4] at lower energies. We may briefly summarize the main features of the observed behaviour of the cross section  $\sigma(\gamma^*p \rightarrow \rho p)$  as follows:

- (i)  $\sigma \sim 1/Q^5$  for  $7 < Q^2 < 30 \text{ GeV}^2$ .
- (ii)  $\sigma \sim W^{0.8}$  for  $12 < W < 140 \text{ GeV}$ .<sup>2</sup>
- (iii)  $\sigma_L/\sigma_T \sim 2 - 4$  weakly rising with  $Q^2$  for  $6 < Q^2 < 20 \text{ GeV}^2$ .
- (iv)  $d\sigma/dt \sim e^{bt}$  with  $b \simeq 5 - 6 \text{ GeV}^{-2}$  for  $Q^2 > 10 \text{ GeV}^2$ ,  
as compared to  $b \simeq 9 \text{ GeV}^{-2}$  for  $Q^2 = 0$ .

As usual,  $Q^2$  is the virtuality of the photon,  $W$  is the centre-of-mass energy of the  $\gamma^*p$  system and  $t$  is the square of the four-momentum transfer. The  $\rho$  meson is observed through its  $2\pi$  decay. If there are sufficient events, then the angular distribution of the decay products allows the measurement of the components  $\sigma_L$  and  $\sigma_T$  of the cross section, which describe  $\rho$  production in longitudinally and transversely polarised states respectively. As we shall see, the measurement of the  $Q^2$  dependence of  $\sigma_L/\sigma_T$  is particularly informative. The present data, (iii), have large errors, but already indicate the general trend.

Observations (ii) and (iv) imply the validity of perturbative QCD for the description of high energy  $\rho$  electroproduction. Observation (iv) means that the size of the system (the  $\gamma^* \rightarrow \rho$  Pomeron vertex) decreases with  $Q^2$ , and that at large  $Q^2$  we do indeed have a short-distance interaction so that perturbative QCD is justified. In fact the measurement of the slope  $b \simeq 5 - 6 \text{ GeV}^{-2}$  is approximately equal to that expected from the size of the proton, which is consistent with the hypothesis that at large  $Q^2$  the size of the  $\gamma^* \rightarrow \rho$  vertex is close to zero. From observation (ii) we see that the exponent of the  $\sigma \sim W^n$  behaviour has changed from the ‘soft’ pomeron value  $n = 4(\alpha_P(\bar{t}) - 1) \simeq 0.2^3$  observed in  $\rho$  photoproduction ( $Q^2 = 0$ ), to a value  $n = 4\lambda \simeq 0.8$  at high  $Q^2$  which is consistent with the gluon density  $xg \sim x^{-\lambda}$  extracted<sup>4</sup> from the observed QCD scaling violations of  $F_2$ . Moreover it is in line with the  $\sigma \sim W^{0.8}$  behaviour observed in  $J/\psi$  photoproduction, where perturbative QCD is expected to be applicable due to the sizeable charm quark mass.

Here we explore the implications of all the observed properties (i)–(iv) for the QCD description of  $\rho$  electroproduction at HERA. Before we present our detailed study, it is useful to give a brief overview of the situation. We begin with the  $Q^2$  dependence of  $\sigma(\gamma^*p \rightarrow \rho p)$ . We will

<sup>2</sup>This behaviour is observed from the NMC experiment at  $W \simeq 13 \text{ GeV}$  right through the HERA energy range, 40–140 GeV.

<sup>3</sup>Corresponding to  $\alpha_P(0) \simeq 1.08$ .

<sup>4</sup>The MRS parton sets which best describe the recent HERA measurements of  $F_2$  [5], and other data, are MRS(A') [6] and MRS(R2) [7]. For these the effective value of  $\lambda$  increases from about 0.2 to 0.3 as  $Q^2$  increases from 10 to 50  $\text{GeV}^2$ .

show that for  $\rho$  meson electroproduction at high  $Q^2$ , perturbative QCD should be applicable to  $\sigma_T$ , as well as  $\sigma_L$ . The leading order perturbative QCD prediction for electroproduction in longitudinally polarised states is [8, 9]

$$\sigma_L \sim \frac{[xg(x, Q^2)]^2}{Q^6} \sim \frac{(Q^2)^{2\gamma}}{Q^6} \sim \frac{1}{Q^{4.8}} \quad (1)$$

for  $Q^2 \gg m_\rho^2$ , where  $x = Q^2/W^2$  and  $\gamma$  is the anomalous dimension of the gluon density,  $xg(x, Q^2) \sim (Q^2)^\gamma$ . For the relevant range of  $x$ ,  $10^{-3} \lesssim x \lesssim 10^{-2}$ , we have taken<sup>5</sup>, for the purposes of illustration, the representative average value  $\gamma = 0.3$ . So the QCD prediction for  $\sigma_L$  is consistent with the  $Q^2$  behaviour of the data. This is not the case for  $\sigma_T$ . The prediction for  $\sigma_T$  appears to be too small and to fall too rapidly with increasing  $Q^2$ . If only the leading twist component of the light-cone wave function<sup>6</sup> of the  $\rho$  is taken into account then

$$\sigma_T \sim \frac{m^2}{Q^2} \sigma_L \sim \frac{1}{Q^{6.8}} \quad (2)$$

where  $m$  is the current (light) quark mass. Although the leading twist is specified by the QCD sum rules, the next twist is not known. However, we can make reasonable assumptions to estimate its effect. We find that its inclusion has the effect of replacing  $m^2$  in (2) by a factor of the order of  $m_\rho^2$ . Even considering the uncertainties, the value predicted for  $\sigma_L/\sigma_T$  is still much too big and has the wrong  $Q^2$  dependence in comparison with the data. We elaborate the above arguments in section 2.

It is frequently claimed that perturbative QCD is not applicable for  $\sigma_T$  and that its behaviour is of non-perturbative origin, see, for example, ref. [9]. But in this case we would expect the same slope  $b$  as in photoproduction and a ‘soft’  $W^{0.2}$  behaviour. Moreover, non-perturbative QCD predicts a  $1/Q^8$  or stronger fall-off of  $\sigma_T$  with increasing  $Q^2$ . Recall that these features are not observed in the data. A further discussion of the non-perturbative approach is given in section 3.

Here we present a resolution of the problem, which is based on the application of the hadron-parton duality hypothesis to the production of open  $q\bar{q}$  pairs. First we recall the hadron-parton duality hypothesis for the process  $e^+e^- \rightarrow$  hadrons. In this case the hypothesis gives

$$\left\langle \sum_h \sigma(e^+e^- \rightarrow \gamma^* \rightarrow h) \right\rangle_{\Delta M^2} \simeq \left\langle \sum_q \sigma(e^+e^- \rightarrow \gamma^* \rightarrow q\bar{q}) \right\rangle_{\Delta M^2}, \quad (3)$$

that is the total hadron production ( $h = \rho, \omega \dots$ ) averaged over a mass interval  $\Delta M^2$  (typically  $\sim 1 \text{ GeV}^2$ ) is well represented by the partonic cross section. This duality has been checked [10]

<sup>5</sup>From the most recent set of partons [6, 7] we find  $\gamma \simeq 0.25$  rising to  $\gamma \simeq 0.4$  as  $x$  decreases from  $10^{-2}$  to  $10^{-3}$  for  $Q^2 \approx 10 \text{ GeV}^2$ . Of course in the numerical analysis of section 6 the true  $x$  and  $Q^2$  dependence of  $\gamma$  is automatically included.

<sup>6</sup>The twist of the  $\rho$  wave function should not be confused with that of the operator which corresponds to the  $\gamma p$  amplitude.

down to the lowest values of  $\sqrt{s}$ . We may therefore expect the duality to apply to diffractive  $\rho$  electroproduction for  $q\bar{q}$  produced in the invariant mass interval containing the  $\rho$  meson,  $M^2 \lesssim 1 - 1.5 \text{ GeV}^2$ . In this domain the more complicated partonic states ( $q\bar{q} + g$ ,  $q\bar{q} + 2g$ ,  $q\bar{q} + q\bar{q}$ , ...) are heavily suppressed, while on the hadronic side the  $2\pi$  (and to a lesser extent the  $3\pi$ ) states are known to dominate. Thus for low  $M^2$  we mainly have

$$\gamma^* \rightarrow q\bar{q} \rightarrow 2\pi \quad (4)$$

or in other words

$$\sigma(\gamma^* p \rightarrow \rho p) \simeq 0.9 \sum_{q=u,d} \int_{M_a^2}^{M_b^2} \frac{d\sigma(\gamma^* p \rightarrow (q\bar{q})p)}{dM^2} dM^2 \quad (5)$$

where the limits  $M_a^2$  and  $M_b^2$  are chosen so that they appropriately embrace the  $\rho$ -meson mass region with  $M_b^2 - M_a^2 \sim 1 \text{ GeV}^2$ . The factor 0.9 is included to allow for  $\omega$  production. This duality model is predictive. In section 4 we present the QCD formula for open  $q\bar{q}$  electroproduction via two gluon exchange, and in section 5 we discuss their general structure. In particular we show how the scale dependence of the gluon density softens the  $\sigma_L/\sigma_T \sim Q^2$  growth with increasing  $Q^2$ . The numerical predictions are presented in section 6. There we calculate diffractive  $u\bar{u}$  and  $d\bar{d}$  electroproduction and use the duality hypothesis to make detailed predictions of the  $Q^2$  dependence of both  $\sigma_L$  and  $\sigma_T$  for  $\rho$  meson electroproduction at HERA; results whose general structure was anticipated in the discussion of section 5.

In short, we argue that the convolution of the  $q\bar{q}$  wave function (produced by the  $\gamma^*$ ) with any reasonable  $\rho$  meson wave function would yield a prediction for  $\sigma_T$  which is in disagreement with the data. Rather we claim that  $\rho$  electroproduction proceeds via *open*  $u\bar{u}$ ,  $d\bar{d}$  production at low  $M^2$ , which has a different structure. Some long time after the interaction with the proton, confinement distorts the  $q\bar{q}$  state and forces it to be the  $\rho$  meson, as there are no other possibilities. That is the suppression due to the small wave function overlap,  $\langle q\bar{q} | \rho^0 \rangle$ , is not operative. We depict the situation in Fig. 1.

## 2. Standard perturbative approach to the $Q^2$ behaviour of $\sigma_{T,L}(\rho)$

First we wish to sketch the derivation of the perturbative QCD prediction, for  $\sigma_T$  shown in (2),

$$\sigma_T(\gamma^* p \rightarrow \rho p) \sim [xg(x, Q^2)]^2 / Q^8 \quad (6)$$

for  $Q^2 \gg m_\rho^2$ , and to show that it is infrared stable. We must therefore study the  $\gamma^* \rightarrow \rho$  Pomeron vertex (or so-called impact factor) of Fig. 1(a), which we denote by  $J_T$ . We shall also consider  $J_L$ . The factors are given by the convolution of the wave functions  $\psi_\gamma(q\bar{q})$  and  $\psi_\rho(q\bar{q})$ . It is found that [9, 11]

$$J_i = f_\rho \int \frac{dz dk_T^2}{\varepsilon^2 + k_T^2} \psi_\rho^i(z, k_T^2) B_i \quad (7)$$

with  $i = T$  or  $L$ . The quantity  $f_\rho$  is the  $\rho$  meson decay constant and the term  $\varepsilon^2$  in the quark propagator is

$$\varepsilon^2 = z(1-z)Q^2 + m^2 \quad (8)$$

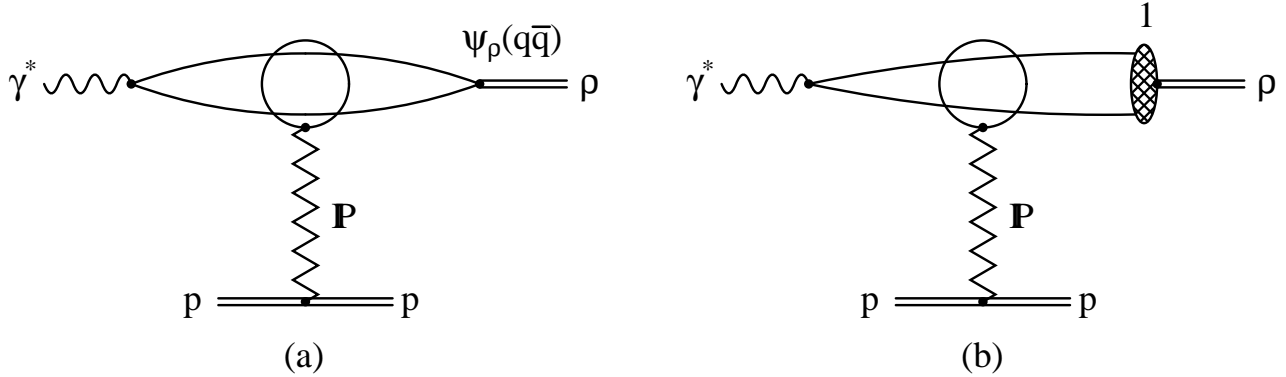


Figure 1: Alternative mechanisms for  $\rho$  meson electroproduction: (a) involves a convolution of the  $\psi_\gamma(q\bar{q})$  and  $\psi_\rho(q\bar{q})$  wave functions, whereas (b) is based on open  $q\bar{q}$  production and parton-hadron duality. At high  $Q^2$  the ‘Pomeron’ exchange in this picture really stands for the exchange of two gluons in the  $t$  channel.

where  $m$  is the current quark mass.  $B_i$  are the helicity factors<sup>7</sup> coming from the quark loop, see Fig. 1(a),

$$B_L = 2z(1-z)\sqrt{Q^2}, \quad (9)$$

$$B_T = -m. \quad (10)$$

$\psi_\rho(z, k_T^2)$  is the momentum representation of the  $\rho$  meson wave function;  $z$  and  $\mathbf{k}_T$  are the Sudakov and transverse momentum components carried by one of the quarks with respect to the photon. The other quark has components  $1-z$  and  $-\mathbf{k}_T$ .

The wave functions  $\psi_\rho^{L,T}$  decrease slowly with  $k_T^2$  and the convergence of the integral in (7) is provided only by the denominator  $\varepsilon^2 + k_T^2$ . We therefore introduce an integrated wave function

$$\phi_\rho^i(z) \equiv \int^{\varepsilon^2} dk_T^2 \psi_\rho^i(z, k_T^2) \quad (11)$$

defined by the scale  $\mu^2 = \varepsilon^2$  at which the integral ceases to converge. The quantities  $\phi_\rho^i$  are called the leading twist light-cone  $\rho$  meson wave functions and have been well studied in the framework of QCD sum rules [12, 13]. As  $Q^2 \rightarrow \infty$  (that is  $\varepsilon^2 \rightarrow \infty$ ) we have

$$\phi_\rho^i(z) \rightarrow 6z(1-z) \quad (12)$$

for both  $i = T, L$ . Their behaviour at finite scales can be found in Refs. [12, 13], but in any case the  $\phi_\rho$  vanish at least as fast as  $z$  as  $z \rightarrow 0$  and  $1-z$  as  $z \rightarrow 1$ . We may rewrite the impact factors (7) in terms of the integrated wave functions  $\phi_\rho^i(z)$ . We obtain

$$J_i \approx f_\rho \int \frac{dz}{\varepsilon^2} \phi_\rho^i(z) B_i. \quad (13)$$

<sup>7</sup>The vertex satisfies  $s$  channel (quark) helicity conservation. In general for  $t \neq 0$  we would also have off-diagonal helicity factors,  $B(\gamma_T, \rho_L)$  and  $B(\gamma_L, \rho_T)$ .

Finally, we must convolute  $J_i$  with the  $q\bar{q}$ -proton interaction amplitude  $T$  given by the BFKL Pomeron (or two-gluon exchange ladder). The amplitude  $T$  behaves as

$$\frac{1}{s}\text{Im}T = \sigma_{q\bar{q}-p} \sim \frac{xg(x, \varepsilon^2)}{\varepsilon^2} \sim (\varepsilon^2)^{\gamma-1} \quad (14)$$

where recall that the scale is  $\varepsilon^2 = z(1-z)Q^2 + m^2$ , and where  $\gamma(x)$  is the anomalous dimension of the gluon. Thus the amplitudes for  $\rho$  electroproduction from transversely ( $i = T$ ) and longitudinally ( $i = L$ ) polarised photons are

$$A_i = J_i \otimes T = f_\rho \int \frac{dz}{(\varepsilon^2)^{2-\gamma}} \phi_\rho^i(z) B_i, \quad (15)$$

which yield the following  $Q^2$  behaviour of the cross sections

$$\sigma_T \sim |A_T|^2 \sim (m/(Q^2)^{2-\gamma})^2 \sim m^2/Q^{6.8}, \quad (16)$$

$$\sigma_L \sim |A_L|^2 \sim Q^2(1/(Q^2)^{2-\gamma})^2 \sim 1/Q^{4.8}. \quad (17)$$

For illustration, we have again set the gluon anomalous dimension  $\gamma = 0.3$ . We emphasize that the integral in (15) is convergent for  $A_T$  (for any  $\gamma > 0$ ), as well as for  $A_L$ . Thus  $\varepsilon^2 \sim Q^2$  and perturbative QCD is valid not only for  $\sigma_L$  (where we have additional convergence due to  $B_L \sim z(1-z)$ ), but *also* for  $\sigma_T$ .

We note that while the prediction for the relative  $Q^2$  dependence of  $\sigma_T$  and  $\sigma_L$  is meaningful (although not supported by the data), the value for the ratio

$$\frac{\sigma_T}{\sigma_L} \sim \frac{m^2}{Q^2} \quad (18)$$

(which is in gross disagreement with the data) is not a reliable estimate. The reason is that the current  $u, d$  quark masses are very small ( $m \lesssim 7$  MeV) and that therefore we must consider how the non-leading twist contribution to  $\psi_\rho^T(z, k_T^2)$  will modify the prediction for  $\sigma_T$ . The non-leading twist is not known. However, it is reasonable to assume that instead of two variables, the  $\rho$  wave function  $\psi_\rho^T$  depends on only one variable, namely the invariant mass of the  $q\bar{q}$  pair<sup>8</sup>

$$M^2 = \frac{k_T^2}{z(1-z)}, \quad (19)$$

where we neglect  $m^2$ . Then, after some algebra, it is possible to show that the impact factor  $J_T$  can be written in the form of (15) with  $\phi_\rho^T = 6z(1-z)$ , and that the helicity factor becomes

$$B_T = -\frac{1}{2} m_\rho [z^2 + (1-z)^2], \quad (20)$$

rather than the very small ‘leading-twist’ prediction given in (10). The reason that we still obtain a definite prediction for  $J_T$ , again in terms of  $f_\rho$ , is due to the fact that this same non-leading twist component of  $\psi_\rho^T$  describes the decay  $\rho_T \rightarrow e^+e^-$ , that is the  $k_T$  integral over the

---

<sup>8</sup>This hypothesis is very natural from a dispersion relation viewpoint [14].

quark loop describing the  $\rho_T$  decay is the same integral that occurs in the impact factor  $J_T$  for  $Q^2 \gg m_\rho^2$ . In this way we are able to normalise the non-leading twist to the observed width of the decay, that is to the decay constant  $f_\rho$ .

If we estimate the  $\rho$  electroproduction amplitude  $A_T$  of (15) using the modified form (20) of  $B_T$  then we obtain

$$\frac{\sigma^T}{\sigma^L} = c \frac{m_\rho^2}{Q^2} \quad (21)$$

with  $c \sim 2$ . The precise value of  $c$  depends on the actual forms of  $\phi_\rho^{T,L}(z)$  at the experimentally relevant scales,  $\mu^2 \sim 10 \text{ GeV}^2$ , which are far from the asymptotic region where  $\phi_\rho^{T,L}(z) = 6z(1-z)$ . In our approximate estimate of  $c \sim 2$  we have used the  $\phi_\rho^{T,L}(z)$  wave functions of ref. [13]. Although a considerable improvement on (18), the prediction (21) for the ratio  $\sigma^T/\sigma^L$  is still much smaller than the observed ratio, and as before decreases more rapidly with  $Q^2$  than indicated by the data [1, 2, 4]. In short, the standard perturbative QCD predictions for  $\sigma_T(\gamma^*p \rightarrow \rho p)$  are not in agreement with the observations.

### 3. Non-perturbative approach to the $Q^2$ dependence of $\sigma_T(\rho)$

It has been argued that the main contribution to  $\sigma_T$  comes from the non-perturbative region [9]. Let us disregard the fact that the perturbative integral (15) is convergent for  $\sigma_T$  and suppose that non-perturbative effects dominate. In order to obtain non-perturbative contributions associated with small ( $\sim \mu^2$ ) virtualities, we must get contributions from the end-point regions of integration

$$z \lesssim \mu^2/Q^2 \quad \text{and} \quad 1-z \lesssim \mu^2/Q^2. \quad (22)$$

Only then will we sample small scales  $\varepsilon^2 \sim \mu^2$  and large distances  $\rho \sim 1/\varepsilon \sim 1/\mu$ . However, for large distances the quark effectively has a constituent mass  $m_q \sim \frac{1}{2}m_\rho$  and the non-relativistic wave function,  $\phi_\rho^T(z) \sim \delta(z - \frac{1}{2})$ , is appropriate. Certainly  $\phi_\rho^T(z)$  decreases exponentially, or at least as a large power, as  $z \rightarrow 0$  or  $z \rightarrow 1$ . Thus the contribution from the regions (22) should be strongly suppressed. Even if  $\phi_\rho^T(z) \sim z(1-z)$ , as in (12), we would obtain from (13) with  $\varepsilon \sim \mu$

$$\sigma_{T(\text{non-pert.})} \sim \left[ \frac{1}{\mu^2} \int_0^{\mu^2/Q^2} dz \phi_\rho^T(z) B_T \right]^2 \sim \frac{1}{Q^8}. \quad (23)$$

Thus for the actual non-perturbative prediction we would expect an even faster fall-off with increasing  $Q^2$ .

### 4. QCD model for $\sigma_{L,T}(\rho)$ via open $q\bar{q}$ production

The above discussion suggests that the problem in successfully describing  $\rho$  meson electroproduction may be associated with having to convolute with a  $\rho$  meson wave function, which inevitably leads to a form-factor-like suppression of the form  $|\langle q\bar{q}|\rho^0 \rangle|^2 \sim 1/Q^4$ . Here we study an alternative and physically compelling mechanism for  $\rho$  electroproduction based on the production of  $u\bar{u}$  and  $d\bar{d}$  pairs in a broad mass interval containing the  $\rho$  meson. In this mass

interval phase space forces these  $q\bar{q}$  pairs to hadronize dominantly into  $2\pi$  states, with only a small amount of  $3\pi$  production. Moreover, provided the  $q\bar{q}$ -proton interaction does not distort the spin, we expect that the process  $\gamma^* \rightarrow q\bar{q} \rightarrow 2\pi$  will dominantly produce  $2\pi$  systems with  $J^P = 1^-$ . The calculation of the diffractive electroproduction of  $q\bar{q}$  pairs therefore allows, via the parton-hadron duality hypothesis, a detailed prediction of the structure of  $\rho$  meson electroproduction.

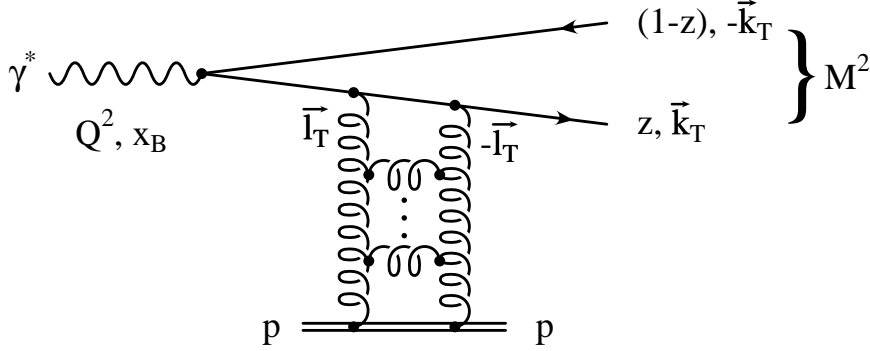


Figure 2: Diffractive open  $q\bar{q}$  production in high energy  $\gamma^*p$  collisions, where  $z$  is the fraction of the energy of the photon that is carried by the quark. The transverse momenta of the outgoing quarks are  $\pm\vec{k}_T$ , and those of the exchanged gluons are  $\pm\vec{\ell}_T$ .

The formula for the diffractive production of open  $q\bar{q}$  pairs is given in ref. [15, 16]. For light quarks we may safely put the current quark mass  $m = 0$ . The process is shown in Fig. 2. We use the same notation as in ref. [15], so the scale at which the gluon distribution is sampled is denoted

$$K^2 = z(1-z)Q^2 + k_T^2 = \frac{k_T^2}{1-\beta}, \quad (24)$$

where the last equality follows since  $z(1-z) = k_T^2/M^2$  and

$$\beta \equiv \frac{Q^2}{Q^2 + M^2}. \quad (25)$$

Note that the scale  $K^2$  plays the role that  $\varepsilon^2$  played for exclusive vector meson production (cf. (8)), and that it determines the transverse distances  $b_T \sim 1/K$  that are typically sampled in the process. It is convenient to replace the  $dk_T^2$  integration over the quark transverse momenta  $k_T$  in formulae (40, 41) in ref. [15] by an integration over  $dK^2$ . Then it is straightforward to show that these formulae giving the  $\gamma_{L,T}^*p \rightarrow (q\bar{q})p$  cross sections in the forward direction ( $t = 0$ ) may be written in the form

$$\frac{d^2\sigma_L}{dM^2 dt} = \frac{4\pi^2 e_q^2 \alpha}{3} \frac{Q^2}{(Q^2 + M^2)^4} \int_{K_0^2}^{\frac{1}{4}(Q^2 + M^2)} \frac{dK^2 K^2}{\sqrt{1 - 4K^2/(Q^2 + M^2)}} [I_L(K^2)]^2, \quad (26)$$

$$\frac{d^2\sigma_T}{dM^2 dt} = \frac{4\pi^2 e_q^2 \alpha}{3} \frac{M^2}{(Q^2 + M^2)^3} \int_{K_0^2}^{\frac{1}{4}(Q^2 + M^2)} \frac{dK^2 (1 - 2\beta K^2/Q^2)}{\sqrt{1 - 4K^2/(Q^2 + M^2)}} [I_T(K^2)]^2 \quad (27)$$

where  $\alpha$  is the electromagnetic coupling. The quantities  $I_{L,T}$  are the integrations over the transverse momenta,  $\pm\ell_T$ , of the exchanged gluons (see Fig. 2)

$$I_L(K^2) = K^2 \int \frac{d\ell_T^2}{\ell_T^4} \alpha_S(\ell_T^2) f(x, \ell_T^2) \left( \frac{1}{K^2} - \frac{1}{K_\ell^2} \right), \quad (28)$$

$$I_T(K^2) = \frac{K^2}{2} \int \frac{d\ell_T^2}{\ell_T^4} \alpha_S(\ell_T^2) f(x, \ell_T^2) \left( \frac{1}{K^2} - \frac{1}{2k_T^2} + \frac{K^2 - 2k_T^2 + \ell_T^2}{2k_T^2 K_\ell^2} \right), \quad (29)$$

where  $x = (Q^2 + M^2)/W^2$ ,

$$K_\ell^2 \equiv \sqrt{(K^2 + \ell_T^2)^2 - 4k_T^2 \ell_T^2}, \quad (30)$$

and  $f(x, \ell_T^2)$  is the unintegrated gluon distribution of the proton. We will use formulae (26) and (27) to predict  $\rho$  meson electroproduction. They involve integration over the quark  $k_T^2$  (or  $K^2$ ) and over the  $\ell_T^2$  of the exchanged gluons. As we are dealing with a diffractive process we see that the cross sections have a quadratic sensitivity to the gluon density.

It is useful to inspect the leading  $\ln K^2$  approximation to the  $d\ell_T^2$  integrations of (28) and (29). In this approximation it is assumed that the main contributions to the integrals come from the domain  $\ell_T^2 \lesssim K^2$ , and so on expanding the integrands we obtain

$$I_L^{LLA} = I_T^{LLA} = \frac{\alpha_S(K^2)}{K^2} \int^{K^2} \frac{d\ell_T^2}{\ell_T^2} f(x, \ell_T^2) = \frac{\alpha_S(K^2)}{K^2} xg(x, K^2). \quad (31)$$

By analogy with (14), we see that  $I_{L,T}$  are essentially the cross sections for the  $(q\bar{q})_{L,T}$  interaction with the proton. Of course, in the calculations presented in section 6 we do not use the leading log approximation, but instead we perform the explicit  $d\ell_T^2$  integrations over  $f(x, \ell_T^2) = \partial(xg(x, \ell_T^2))/\partial \ln \ell_T^2$  given in (28) and (29). We treat the infrared region using the linear approximation described in ref. [15] for low  $\ell_T^2$  values (that is  $\ell_T^2 < \ell_0^2$ ). We find stability of the results to reasonable variations of the choice of  $\ell_0^2$ .

## 5. Insight into the structure of the cross sections $\sigma_{L,T}$

In section 6 we show the predictions for the  $Q^2$  behaviour of  $\sigma_L$  and  $\sigma_T$  for  $\rho$  electroproduction, which are obtained from the numerical evaluation of (26) and (27) integrated over the  $\rho$  mass region. However, it is informative to anticipate some of the general features of the results. First we study the infrared convergence of the  $dK^2$  integrations of (26) and (27). We note from the approximate forms of  $I_{L,T}$  in (31) that

$$I_i \sim x^{-\lambda} (K^2)^\gamma / K^2 \quad (32)$$

where  $\lambda$  and  $\gamma$  are the effective exponents of the gluon defined by

$$xg(x, K^2) \sim x^{-\lambda} (K^2)^\gamma. \quad (33)$$

We see that the integration (26) is infrared convergent provided that  $\gamma > 0$  as  $K^2 \rightarrow 0$ , whereas

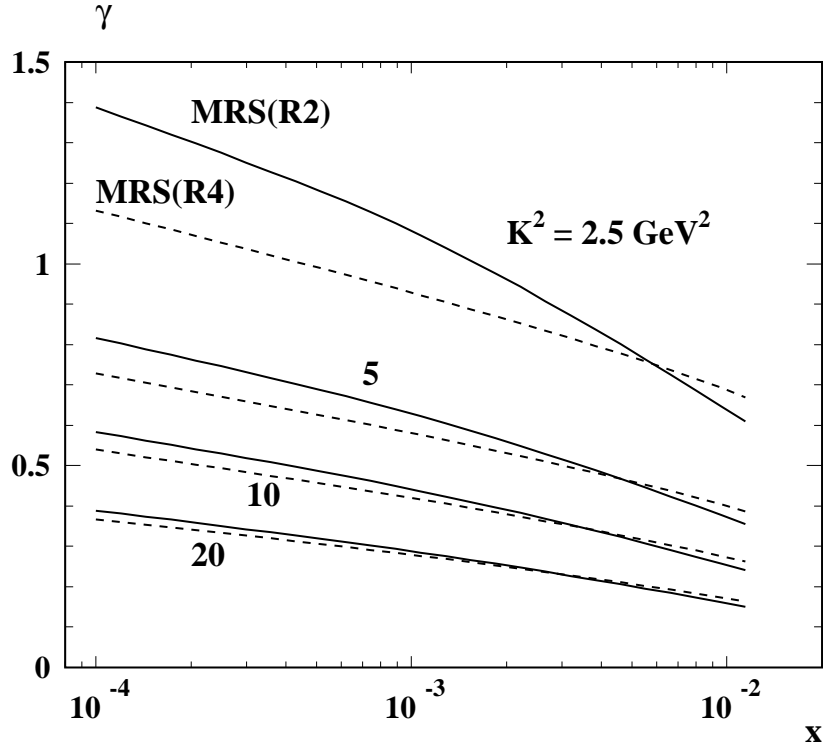


Figure 3: The continuous curves show the effective anomalous dimension  $\gamma$  of the gluon (defined by  $xg(x, K^2) \sim (K^2)^\gamma$ ) determined from the MRS(R2) set of partons [7] for  $K^2 = 2.5, 5, 10$  and  $20 \text{ GeV}^2$ . The dashed curves correspond to the values of  $\gamma$  for the R4 set of partons.

we require  $\gamma > 0.5$  to ensure the convergence of (27). How does the value of  $\gamma$  depend on  $K^2$ ? At high energy  $W$  (that is  $x \approx Q^2/W^2 \rightarrow 0$ ) the gluon  $g(x, K^2)$  increases much faster as  $x$  decreases for large  $K^2$  ( $xg \sim x^{-\lambda}$  with  $\lambda \gtrsim 0.3$ ) than for small  $K^2$ . Thus the effective anomalous dimension  $\gamma$  increases when  $x$  and  $K^2$  decrease. The behaviour is evident in Fig. 3 which shows the values of  $\gamma$  (as a function of  $x$  for selected  $K^2$ ) obtained from two recent sets of partons. For example, let us take a typical value  $x \approx Q^2/W^2 = 10^{-3}$  relevant for the measurements at HERA (say  $Q^2 = 10 \text{ GeV}^2$  and  $W = 100 \text{ GeV}$ ). We see from Fig. 3 that  $\gamma$  increases from 0.3, 0.45, 0.6 to 1 as  $K^2$  decreases from about 20, 10, 5 to  $2.5 \text{ GeV}^2$ . The infrared convergence requirement,  $\gamma > 0.5$ , of (27) is therefore already satisfied when  $K^2$  has decreased to  $8 \text{ GeV}^2$ . In general, the behaviour of  $\gamma$  with  $K^2$  amply provides, via (32), the infrared convergence of (27), as well as of (26). This explains the reason why our numerical evaluation of (27) for  $\sigma_T$  depends only weakly on the infrared cut-off<sup>9</sup>  $K_0^2$ . Indeed integral (26) for  $\sigma_L$  is controlled by contributions close to the upper limit and we expect

$$\frac{d^2\sigma_L}{dM^2 dt} \sim \frac{(Q^2)^{2\gamma-2\lambda}}{Q^6}. \quad (34)$$

This is exactly the same  $Q^2$  behaviour as the prediction (17) for *exclusive*  $\rho_L$  electroproduction;

<sup>9</sup>In section 6 we choose  $K_0 = 0.2 \text{ GeV}$ , the order of the inverse confinement radius  $1 \text{ fm}^{-1}$ .

here we have been more precise and displayed the  $Q^2$  dependence coming from the  $x(\simeq Q^2/W^2)$  behaviour of the gluon. Of course, the result (34) is very approximate and the detailed dependence of the  $Q^2$  behaviour of  $\sigma_L$  (as well as  $\sigma_T$ ) on the properties of the gluon must await the numerical predictions of section 6.

Nevertheless we can take the general discussion further and anticipate the main features of the  $Q^2$  behaviour of the important ratio  $\sigma_L/\sigma_T$ . We first rewrite (26) and (27) in terms of an integration over the angles of the produced  $q\bar{q}$  pair. We use the polar angle  $\theta$  of the outgoing  $q$  in  $q\bar{q}$  rest frame with respect to the incident direction of the proton. Thus we have

$$k_T = \frac{1}{2}M \sin \theta, \quad (35)$$

and the square root in the denominators of (26) and (27) is equal to  $\cos \theta$ . Also the factor in the numerator of (27)

$$1 - 2\beta K^2/Q^2 = \frac{1}{2}(1 + \cos^2 \theta) = |d_{11}^1(\theta)|^2 + |d_{1-1}^1(\theta)|^2, \quad (36)$$

where  $d_{\lambda\mu}^J(\theta)$  are the conventional spin rotation matrices. Then equations (26) and (27) become

$$\frac{d^2\sigma_L}{dM^2 dt} = \frac{4\pi^2 e_q^2 \alpha}{3} \frac{Q^2}{(Q^2 + M^2)^2} \frac{1}{8} \int_{-1}^1 d \cos \theta |d_{10}^1(\theta)|^2 |I_L|^2, \quad (37)$$

$$\frac{d^2\sigma_T}{dM^2 dt} = \frac{4\pi^2 e_q^2 \alpha}{3} \frac{M^2}{(Q^2 + M^2)^2} \frac{1}{4} \int_{-1}^1 d \cos \theta \left( |d_{11}^1(\theta)|^2 + |d_{1-1}^1(\theta)|^2 \right) |I_T|^2, \quad (38)$$

where the dependence on the rotation matrices appropriately reflects the decay of the  $\rho$  meson from longitudinally and transversely polarised states, respectively.

In the limit of no interaction with the proton (that is  $I_L = I_T = \text{constant}$ ) the photon has to produce the  $q\bar{q}$  pair in a pure spin  $J = 1$  state. We immediately find from (37) and (38) that

$$\frac{\sigma_L}{\sigma_T} = \frac{Q^2}{2M^2} \frac{\int d \cos \theta \sin^2 \theta}{\int d \cos \theta (1 + \cos^2 \theta)} = \frac{Q^2}{4M^2}. \quad (39)$$

In the realistic situation, the two-gluon exchange interaction distorts the  $q\bar{q}$  state produced by the ‘heavy’ photon. Some idea of the consequences of this distortion can be anticipated from the leading log approximation (31) for  $I_L$  and  $I_T$ , in which

$$I_L = I_T \sim \frac{(K^2)^\gamma}{K^2} \sim \frac{1}{(\sin^2 \theta)^{1-\gamma}}. \quad (40)$$

We substitute this behaviour into (37) and (38), and project<sup>10</sup> out the spin 1 components of the underlying  $q\bar{q}$  production amplitudes ( $\sim d_{1\lambda}^1(\theta) I(\theta)$  where  $I_L = I_T \equiv I(\theta) \sim (\sin^2 \theta)^{\gamma-1}$ ). We then use the identity

$$\int_0^\pi \sin^p \theta d\theta = \sqrt{\pi} \frac{\Gamma(\frac{1}{2} + \frac{1}{2}p)}{\Gamma(1 + \frac{1}{2}p)} \quad (41)$$

---

<sup>10</sup>To be precise the rotation matrices  $D_{\lambda\mu}^J(\phi, \theta, -\phi)$  form the orthogonal basis and we project out the components  $c(\lambda)$  from the  $q\bar{q}$  amplitudes  $D_{1\lambda}^{1*} I(\theta)$  with the matrix  $D_{1\lambda}^1$ . However, the  $\phi$  integrations are trivial and hence the projection can be done simply in terms of  $d_{1\lambda}^1$ .

to evaluate the projections

$$c(\lambda) = \frac{2J+1}{2} \int d\cos\theta \left( d_{1\lambda}^{J=1}(\theta) I(\theta) \right) d_{1\lambda}^{J=1}(\theta), \quad (42)$$

assuming that  $\gamma$  is a constant over the region of integration. With this assumption we find the interesting result

$$\frac{\sigma_L}{\sigma_T} = \frac{Q^2}{2M^2} \frac{|c(\lambda=0)|^2}{|c(\lambda=1)|^2 + |c(\lambda=-1)|^2} = \frac{Q^2}{M^2} \left( \frac{\gamma}{\gamma+1} \right)^2. \quad (43)$$

The dependence on  $\gamma$  has the effect of masking the  $Q^2$  growth of  $\sigma_L/\sigma_T$ . This can be seen by inspecting Fig. 3 – higher  $Q^2$  means larger  $x$  and both changes imply smaller  $\gamma$ . The projection integrals (42) for the amplitudes (with their linear dependence on  $I_i(\theta)$ ) are more infrared convergent than (37) and (38). Now  $\sigma_T$  (as well as  $\sigma_L$ ) is convergent provided only that  $\gamma > 0$  as  $K^2 \rightarrow 0$  (that is as  $\theta \rightarrow 0$ ). In fact, provided  $x$  remains sufficiently small, both the  $\sigma_L$  and  $\sigma_T$  integrations receive their main contributions from the region  $K^2 \lesssim Q^2/4$ , and so we should insert into (43) the average  $\gamma$  sampled in this  $x, K^2$  domain. Indeed the decrease of  $\gamma$  with increasing  $K^2 \lesssim Q^2/4$  is found to considerably suppress the growth of  $\sigma_L/\sigma_T$  with increasing  $Q^2$ , and to largely remove the gross disagreement of the QCD prediction with the data; see the full numerical calculation presented in section 6. We may turn the argument the other way round. Accurate measurements of the ratio  $\sigma_L/\sigma_T$  as a function of  $Q^2$  will offer an excellent way of constraining the  $K^2$  and  $x$  behaviour of the gluon  $g(x, K^2)$  in the region  $K^2 \lesssim Q^2/4$  and  $x \approx Q^2/W^2$ . Of course result (43), which is based on a constant  $\gamma$ , is oversimplified. It is given only to indicate the general trend. The full calculation of section 6 is performed with a realistic gluon distribution and so automatically allows for the  $K^2$  (and  $x$ ) dependence of  $\gamma$ .

We see that the projection integrals (42) converge in the infrared region of small  $K^2 \approx \frac{1}{4}Q^2 \sin^2\theta$  (that is at small  $\theta$ ) for any  $\gamma > 0$ , even for  $\sigma_T$  (that is for  $c(\lambda = \pm 1)$ ). We have stronger infrared convergence for  $\sigma_L$  or  $c(\lambda = 0)$  due to  $d_{10}^1 = -\sin\theta/\sqrt{2}$ . We also notice that the factor  $I(\theta) = 1/(\sin^2\theta)^{1-\gamma}$ , arising from the  $q\bar{q}$ -proton interaction, gives a strong peak in the forward direction<sup>11</sup>. It means that the distortion caused by the interaction will, in principle, produce higher spin  $q\bar{q}$  states. Most probably the higher spin states at small  $M^2$  are killed by confinement during the hadronization stage as there is insufficient phase space to create  $2\pi$  states with large spin with  $M^2 \lesssim 1 \text{ GeV}^2$ . In any case the higher spin components<sup>12</sup> cannot affect  $\rho$  production, since confinement cannot change the spin of the produced  $q\bar{q}$  state. At higher energies (small  $x$ ) the anomalous dimension  $\gamma$  grows and the function  $I(\theta)$  is not so singular as  $\theta \rightarrow 0$ . Therefore in this energy domain the incoming spin of the  $q\bar{q}$  system is not so contaminated by  $J \neq 1$  components arising from the interaction with the proton. In the black disk limit of the proton when the cross section approaches the saturation (unitarity) limit  $\gamma$  tends to 1 and we come back to pure  $J = 1$   $q\bar{q}$  production.

<sup>11</sup>The height of the peak is limited by the infrared cut-off,  $K_0 = 0.2 \text{ GeV}$ , provided by confinement.

<sup>12</sup>Indeed it will be interesting to study the detailed spin decomposition of  $\gamma^* \rightarrow$  open  $q\bar{q}$  production as a function of  $M^2$ . In this way we can investigate how the QCD ‘Pomeron’ distorts the initial state and how confinement/parton-hadron duality operates in different (relatively small)  $M^2$  regions for the different  $J^P$  states.

## 6. Numerical QCD predictions for $\rho$ electroproduction

We use parton-hadron duality to predict  $\rho$  electroproduction from the QCD formulae for open  $u\bar{u}$  and  $d\bar{d}$  production. To be precise we compute

$$\sigma_{L,T}(\rho) = 0.9 \int_{(0.6 \text{ GeV})^2}^{(1.05 \text{ GeV})^2} dM^2 \frac{d\sigma_{L,T}(J=1)}{dM^2} \quad (44)$$

where  $d\sigma_{L,T}(J=1)/dM^2$  are the spin 1 projections of open  $q\bar{q}$  production of (37) and (38), carried out as described in (42), and where the cross sections have been integrated over  $t$  assuming the form  $\exp(-b|t|)$  with the observed slope  $b = 5.5 \text{ GeV}^{-2}$  [1, 2]. The factor 0.9 is included in (44) to allow for  $\omega$  production. The  $I_L$  and  $I_T$  integrations over the gluon transverse momentum are computed from (28) and (29) as described in ref. [15]. We checked the stability of the results to contributions from the infrared regions of the  $dK^2$  and  $d\ell_T^2$  integrations. First we varied the infrared cut-off around the value  $K_0 = 200 \text{ MeV}$  that we used to evaluate (26) and (27). Second we explored the effect of varying  $\ell_0^2$  around the value  $\ell_0^2 = 1.5 \text{ GeV}^2$  that we used to evaluate the integrals of (28) and (29). Recall that we use the linear approximation described in ref. [15] to evaluate the contribution from the region  $\ell_T^2 < \ell_0^2$ . We found only a weak sensitivity to variation of the choice of  $\ell_0^2$ . For instance reducing  $\ell_0^2$  to  $1 \text{ GeV}^2$  changes the cross sections by less than 5%. We will report on the sensitivity to variation of  $K_0$  at the end of the section.

We begin by taking the gluon distribution from the MRS(R2) set of partons [7], which correspond to a QCD coupling which satisfies  $\alpha_S(M_Z^2) = 0.12$ . The parton set with this QCD coupling, found by global analysis of deep inelastic and related data (including recent HERA measurements of  $F_2$ ), is favoured by the Fermilab jet data with  $E_T < 200 \text{ GeV}$  [7]. We first compare our cross section predictions obtained with this gluon with the data. Then we use different gluon distributions from several recent sets of partons to study the sensitivity of  $\gamma^*p \rightarrow \rho p$  to the behaviour of the gluon.

Note that we use phenomenological gluon distributions which are obtained from global fits to deep inelastic experimental data, rather than “ab initio” distributions calculated from theoretical models. Thus the gluon distributions that we use already incorporate absorptive effects.

There is another crucial ingredient in the calculation of the cross section for diffractive open  $q\bar{q}$  production. Virtual gluon corrections to the process shown in Fig. 2 are surprisingly important. The relevant diagrams are discussed in ref. [15] and lead to  $\pi^2$  enhancements of the  $\mathcal{O}(\alpha_S)$  corrections. If the contributions are resummed they lead to an enhancement of the lowest order result by a factor  $\exp(\alpha_S C_F \pi)$ , the so-called  $K$  factor enhancement, where the colour factor  $C_F = 4/3$ . A similar  $K$  factor is well known in Drell-Yan production, although there the contributions come from different virtual diagrams [15]. For the Drell-Yan process the enhancement can be as much as about a factor of 3. In our case the  $K$  factor can, at present, only be estimated. It proves to be the main uncertainty in the normalization of diffractive  $q\bar{q}$  production. The major ambiguity is associated with the choice of the argument of  $\alpha_S$ . We

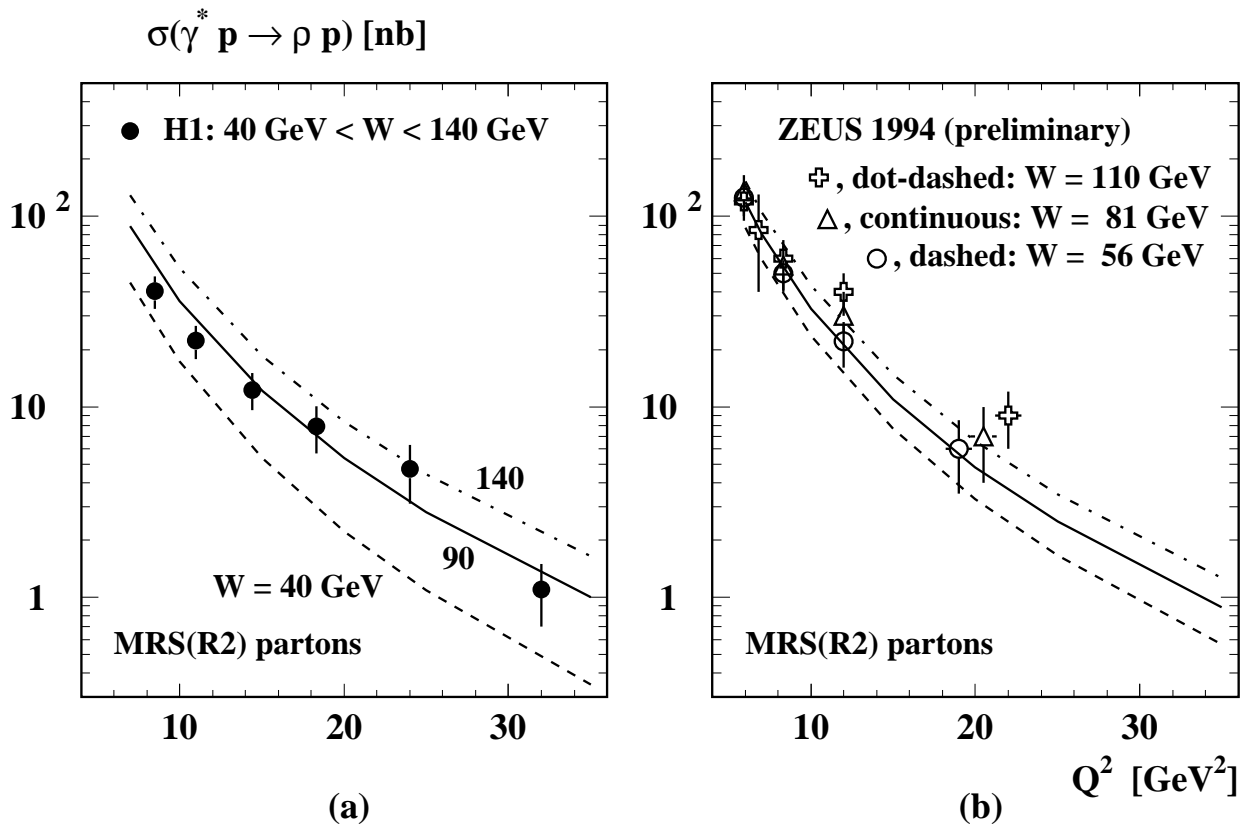


Figure 4: The predicted  $Q^2$  dependence of the cross section for  $\gamma^* p \rightarrow \rho p$  compared with (a) H1 data [1] collected over the energy range  $40 < W < 140$  GeV and (b) preliminary ZEUS data [3] in energy bins with  $\langle W \rangle = 56, 81$  and  $110$  GeV. The QCD curves for the various values of  $W$  are obtained using MRS(R2) partons [7].

take the scale to be  $2K^2$ . Since the  $K^2$  integrations are dominated by contributions towards the upper limit this choice is equivalent to a scale  $\lesssim Q^2/2$ . With this choice we obtain the values of the  $\gamma^* p \rightarrow \rho p$  cross section shown by the curves in Fig. 4, which are in reasonable agreement with the measured values. For our choice of scale the average  $K$  factor for  $\sigma_L$  varies from about 3 to 3.7 for  $Q^2$  going from 25 to 10 GeV<sup>2</sup>, and is about 20–25% larger for  $\sigma_T$  (as in this case somewhat lower  $K^2$  values are sampled). The cross section agreement shown in Fig. 4 corresponds to a physically reasonable choice of scale, and leads to a sensible range of size of the  $K$  factors. It shows that the open  $q\bar{q}$  duality model for  $\rho$  electroproduction is at least consistent with observations. Due to the sensitivity to the choice of scale, clearly the agreement cannot be regarded as confirmation of the approach. Nevertheless, it does imply the existence of a sizeable “ $\pi^2$ ” enhancement of the Born amplitude, as was also found in the Drell-Yan process.

On the other hand the predictions for the  $Q^2$  dependence of the ratio  $\sigma_L/\sigma_T$  have much less ambiguity. The calculations are compared with the measurements at HERA in Fig. 5. The agreement with the data shows a dramatic improvement over the QCD expectations which

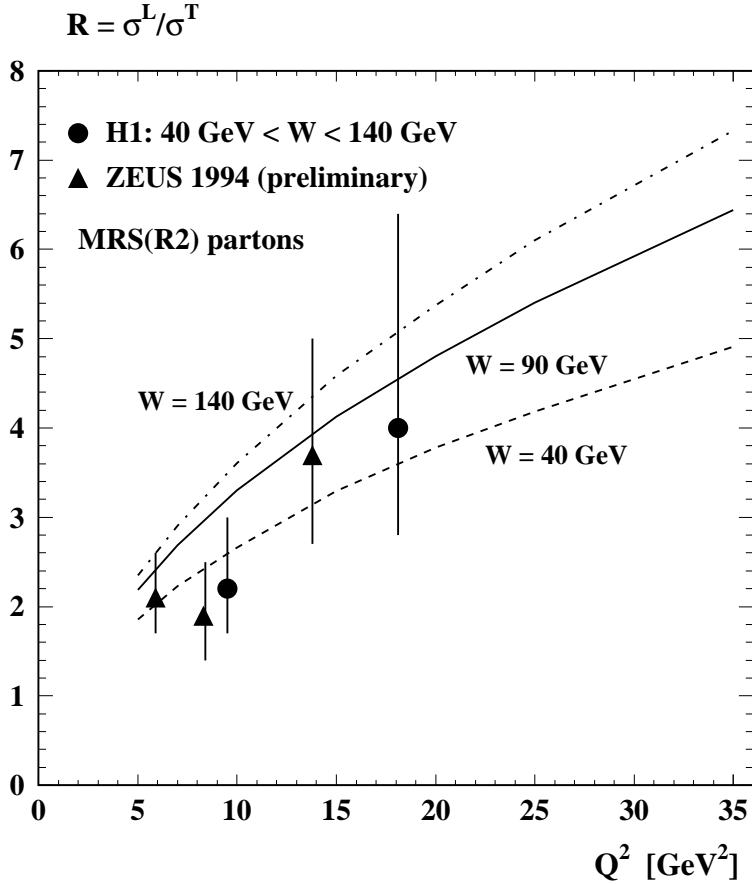


Figure 5: The  $Q^2$  dependence of the QCD predictions for the ratio  $\sigma_L/\sigma_T$  of the electroproduction of  $\rho$  mesons ( $\gamma^*p \rightarrow \rho p$ ) in longitudinal and transverse polarisation states compared with the most recent H1 [1] and ZEUS [3] data. MRS(R2) partons [7] are used.

involve convolution with the  $\rho$  meson wave function. The small  $x$  behaviour of the gluon plays a crucial role in masking the  $Q^2$  increase anticipated in these earlier predictions of the ratio.

The dependence on the gluon is seen in Fig. 6 which compares the  $Q^2$  behaviour for  $\sigma_L/\sigma_T$  at  $W = 90$  GeV for the gluon distribution of several recent sets of partons (MRS(A') [6], GRV [17], MRS(R2) [7]). We stress that the normalization of the QCD predictions for the cross section are dependent on the choice of the mass interval embracing the  $\rho$  meson and on the estimate of the  $K$  factor enhancement. On the other hand the ratio  $\sigma_L/\sigma_T$  is not so sensitive to these ambiguities. At this stage it is relevant to study the stability of the results to variation of the infrared cut-off  $K_0$ . This we also show in Fig. 6, where we present QCD predictions based on MRS(R2) partons for two different choices of  $K_0$ . We see that the cross section is hardly changed while the ratio  $\sigma_L/\sigma_T$  increases a little when  $K_0$  is increased from 200 to 300 MeV. Such a result is to be anticipated as  $\sigma_T$  samples, on average, smaller  $K^2$  values than  $\sigma_L$ . However, we see that the sensitivity of the predictions for  $\sigma_L/\sigma_T$  to the value of  $K_0$  is sufficiently weak so that measurements of the ratio can give a reliable probe of the gluon.

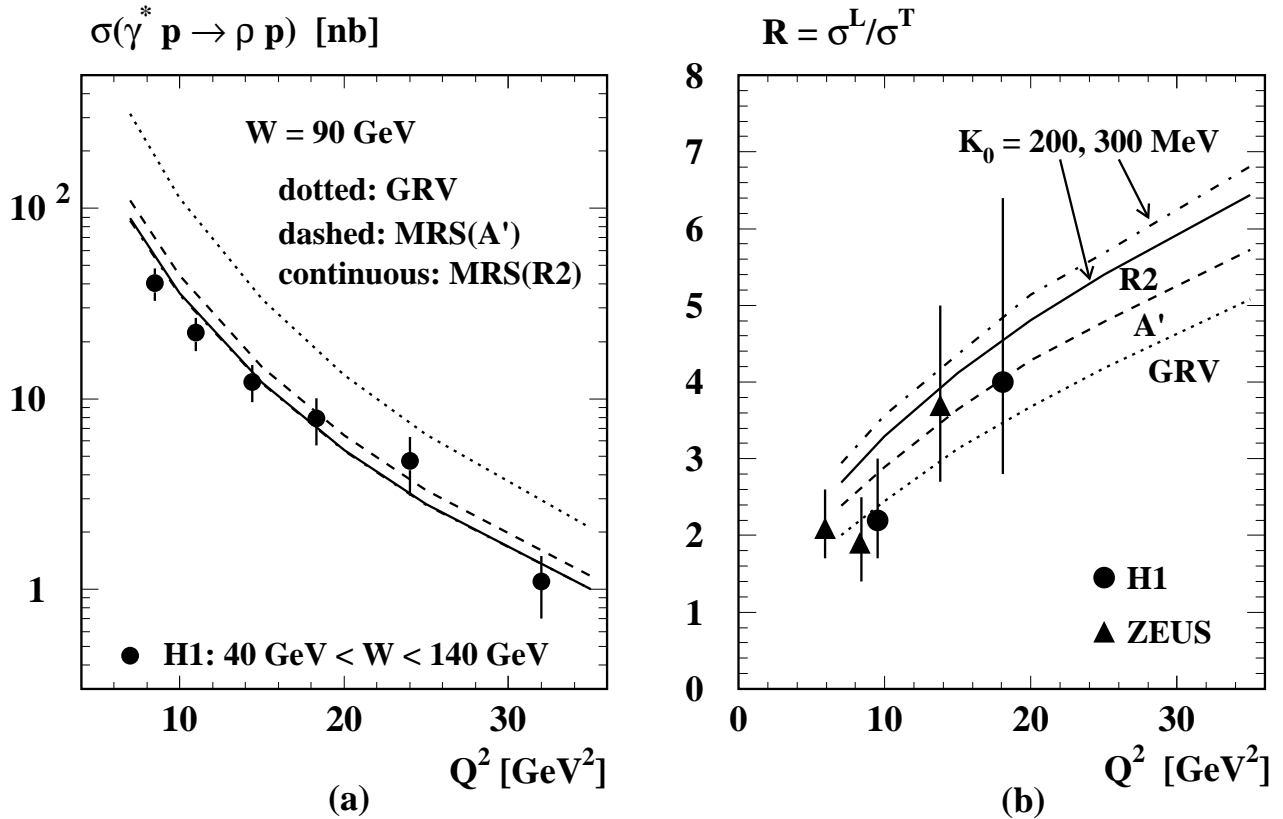


Figure 6: The QCD predictions for  $W = 90$  GeV based on three recent sets of partons [6, 7, 17] compared with the recent HERA data [1, 3]. We also show the sensitivity of the predictions using the MRS(R2) partons to the choice of the cut-off  $K_0$ ; the dot-dashed curves correspond to  $K_0 = 300$  MeV whereas all other curves correspond to  $K_0 = 200$  MeV. The dot-dashed curve in (a) essentially coincides with the continuous curve which demonstrates the insensitivity of the cross section prediction to the value of  $K_0$ , whereas we see that the ratio  $\sigma_L/\sigma_T$  of (b) has some dependence.

## 7. Conclusions

We have shown that the diffractive electroproduction of  $\rho$  mesons at high  $Q^2$  can be described by perturbative QCD. Indeed, since  $\rho$  production in both longitudinally and transversely polarised states is being measured at HERA with better and better precision, the process  $\gamma^* p \rightarrow \rho p$  can serve as an excellent testing ground for QCD. Moreover, we have shown that it also provides a sensitive probe of the small  $x$  behaviour of the gluon distribution.

The validity of perturbative QCD is ensured by the large value of  $Q^2$ . This is already suggested by several features of the existing data [1, 2, 4]. However, the measurements of the

ratio  $\sigma_L/\sigma_T$  do not support the behaviour,

$$\frac{\sigma_L}{\sigma_T} \sim \frac{Q^2}{2m_\rho^2}, \quad (45)$$

predicted from QCD by convoluting  $\gamma^* \rightarrow q\bar{q}$  diffractive production with our knowledge of the  $\rho$  meson wave function. The main problem is that the predictions for  $\sigma_T$  are too small and fall off too quickly with increasing  $Q^2$ . We showed that a non-perturbative approach to  $\sigma_T$  does not resolve the conflict with the data. Rather we argued that on account of the low mass of the  $\rho$  meson the convolution with the wave function should be omitted. The  $u\bar{u}$  or  $d\bar{d}$  pairs produced in the  $\rho$  mass region have, because of phase space restrictions, little alternative but to hadronize as  $2\pi$  states. Thus a more appropriate approach to  $\rho$  electroproduction is to apply the parton-hadron duality hypothesis to open  $u\bar{u}$  and  $d\bar{d}$  production. Indeed we found that this model gives a good description of all of the features observed for diffractive  $\rho$  electroproduction at HERA, including in particular the  $Q^2$  behaviour of  $\sigma_L/\sigma_T$ . To gain insight into expectations of the model, we first made a simple estimate based on assuming a constant anomalous dimension  $\gamma$ . We found

$$\frac{\sigma_L}{\sigma_T} = \frac{Q^2}{M^2} \left( \frac{\gamma}{\gamma + 1} \right)^2, \quad (46)$$

where  $M$  is the invariant mass of the  $q\bar{q}$  pair and  $\gamma$  is the effective anomalous dimension of the gluon defined by  $xg(x, K^2) \sim (K^2)^\gamma$ , where the typical  $K^2$  sampled is  $K^2 \lesssim Q^2/4$  (approximated to be the same for both  $\sigma_L$  and  $\sigma_T$ ). The decrease of  $\gamma$  with increasing  $Q^2$  masks the strong growth shown in (45). Of course result (46) is greatly oversimplified but it gives a good idea of the crucial role played by the gluon distribution. In Figs. 4–6 we showed the results of the full calculation. The computation is based on a measured gluon distribution and so automatically allows for the appropriate  $K^2$  and  $x$  dependence of  $\gamma$ . The figures compare the detailed predictions of the model with the measurements of diffractive  $\rho$  electroproduction at HERA. The main uncertainty is in the normalization of the cross section. One source is in the choice of the width of the  $\Delta M^2$  interval over which to apply the duality hypothesis. The second is associated with the  $K$  factor enhancement which arises from virtual gluon corrections to open  $q\bar{q}$  production. The normalization is sensitive to the choice of scale used as the argument of  $\alpha_S$  in the calculation of the  $K$  factor. The data show evidence for a  $K$  factor of about 3–4, comparable in size to the  $K$  factor enhancement established for Drell-Yan production.

The QCD model prediction of the ratio  $\sigma_L/\sigma_T$  is essentially free of the above ambiguities. Fig. 6 shows that precise measurements of the ratio for  $\rho$  electroproduction at different values of  $Q^2$ , and the  $\gamma^*p$  c.m. energy  $W$ , will provide a valuable probe of the behaviour of the gluon distribution  $g(x, K^2)$  in the kinematic domain  $x \approx Q^2/W^2$  and  $K^2 \lesssim Q^2/4$ .

## Acknowledgements

We thank E.M. Levin and R.G. Roberts for useful discussions and H. Abramowicz, A. Caldwell, B. Clerbaux and A. De Roeck for information about the HERA data. MGR thanks the Royal Society for a Fellowship grant and TT thanks the UK Particle Physics and Astronomy Research Council for support. This research was also supported in part (MGR) by the Russian Fund of Fundamental Research 96 02 17994.

## References

- [1] H1 collaboration: S. Aid *et al.*, *Nucl. Phys.* **B468** (1996) 3.
- [2] ZEUS collaboration: M. Derrick *et al.*, *Phys. Lett.* **B356** (1995) 601.
- [3] ZEUS collaboration, submitted paper pa02-028 to the *XXVIII. International Conference on High Energy Physics, Warsaw, July 1996*.
- [4] NMCollaboration: M. Arneodo *et al.*, *Nucl. Phys.* **B429** (1994) 503.
- [5] H1 collaboration: S. Aid *et al.*, *Nucl. Phys.* **B470** (1996) 3;  
ZEUS collaboration: M. Derrick *et al.*, *Z. Phys.* **C69** (1996) 607;  
DESY-96-076 and hep-ex/9607002.
- [6] A.D. Martin, R.G. Roberts and W.J. Stirling, *Phys. Lett.* **B354** (1995) 155.
- [7] A.D. Martin, R.G. Roberts and W.J. Stirling, Durham preprint DTP/96/44,  
RAL-TR-96-037, hep-ph/9606345, *Phys. Lett.* **B** (in press).
- [8] M.G. Ryskin, *Z. Phys.* **C57** (1993) 89.
- [9] S.J. Brodsky *et al.*, *Phys. Rev.* **D50** (1994) 3134.
- [10] E.C. Poggio, H.R. Quinn and S. Weinberg, *Phys. Rev.* **D13** (1976) 1958;  
Yu. L. Azimov *et al.*, *Z. Phys.* **C27** (1985) 65; *ibid.* **C31** (1986) 213;  
Yu. L. Dokshitzer, V.A. Khoze and S.I. Troyan, *Z. Phys.* **C55** (1992) 107.
- [11] D.Yu. Ivanov, *Phys. Rev.* **D53** (1996) 3564;  
I.F. Ginzburg, D.Yu. Ivanov and V.G. Serbo, Novosibirsk preprint IM-TP-208, Aug. 1995  
and hep-ph/9508309;  
I.F. Ginzburg and D.Yu. Ivanov, hep-ph/9604437, *Phys. Rev.* **D** (in press).
- [12] V.L. Chernyak and I.R. Zhitnitsky, *Phys. Rep.* **112** (1984) 173.
- [13] P. Ball and V. Braun, *Phys. Rev.* **D54** (1996) 2182.

- [14] V.N. Gribov, *Sov. Phys. JETP* **30** (1970) 709;  
L.L. Frankfurt and M.I. Strikman, *Phys. Lett.* **B65** (1976) 51.
- [15] E.M. Levin, A.D. Martin, M.G. Ryskin and T. Teubner, Durham preprint DTP/96/50, hep-ph/9606443, *Z. Phys.* **C** (in press).
- [16] N.N. Nikolaev and B.G. Zakharov, *Z. Phys.* **C49** (1991) 607;  
*Phys. Lett.* **B260** (1991) 414; *Z. Phys.* **C53** (1992) 331;  
J. Bartels, H. Lotter and M. Wüsthoff, *Phys. Lett.* **B379** (1996) 239;  
E. Gotsman, E.M. Levin and U. Maor, CBPF-NF-021/96, TAUP-2338-96 and hep-ph/9606280.
- [17] M. Glück, E. Reya and A. Vogt, *Z. Phys.* **C67** (1995) 433.